JOURNAL OF APPLIED PHYSICS **109**, 054904 (2011)

Local heating of heterogeneous current-carrying conductors

Yu. Dolinsky[a)] and T. Elperin[a)]
The Pearlstone Center for Aeronautical Engineering Studies, Department of Mechanical Engineering, Ben-Gurion University of the Negev, P. O. B. 653, Beer-Sheva 84105, Israel

(Received 23 March 2010; accepted 16 December 2010; published online 8 March 2011)

We study the heating of current-carrying conductors with inclusions when the kinetic coefficients of inclusions are different from those of the conductor. It is shown that if the surface temperature of the conductor is maintained constant and the thermal conductivity of the inclusion is higher than the thermal conductivity of the conductor, the temperature distribution in the vicinity of the inclusion is strongly different from the temperature distribution in a homogeneous conductor. Depending on the parameters of the system the temperature at the location of an inclusion can be two times higher than the temperature at the same location without an inclusion. We investigate the behavior of the temperature difference as a function of the distance between the center of the spherical inclusion and the conductor's surface. We analyze different components of Joule heating, which are associated with the change of the configuration of the electric current caused by the inclusion and with the change of temperature distribution caused by different thermal conductivities of the conductor and inclusion. We consider a stationary regime of conductor heating whereby the surface temperature of the conductor is kept constant in time, and the case of a thermally insulated conductor. It is demonstrated that in the latter case the temperature of the inclusion can be considerably lower than the surface temperature of the conductor. © *2011 American Institute of Physics*. [doi:10.1063/1.3549608]

I. INTRODUCTION

Numerous experimental investigations (see, e.g., Refs. 1–5) have demonstrated that the action of an electric current on conducting materials offers an efficient method for changing the internal structure of materials. In particular, it was shown that the electric current alters the grain structure in the materials,[1–3] reduces resistance of the conductors,[2,3] causes reduction of crystallization temperature,[4] leads to formation of twinning centers,[5] etc. All of these effects were observed in a wide range of electric current densities. In Ref. 1 the magnitude of the electric current densities whereby these effects were observed varied in the range of $4-400\ \mathrm{mA/cm^2}$ while in Ref. 4 the electric current density was of the order of $10^5\ \mathrm{A/cm^2}$. Different effects are observed in current-carrying conductors due to a multitude of associated physical mechanisms when their composition is inhomogeneous. One of these mechanisms is associated with the change of the work of formation of the nucleus of the new phase when electric conductivities of the conductor and the new phase are different. This mechanism in systems with different geometries was considered in a number of theoretical studies.[6–10] Another mechanism which must be taken into account in the analysis of the effect of the electric current on structural material changes in conductors is Joule heating. A separate investigation of the effect of Joule heating on the temperature distribution in a heterogeneous conductor with inclusions, e.g., inclusions of new phase, large grains of impurities or admixtures, is required in order to analyze structural changes in current-carrying conductors. Despite the obvious importance of such an investigation, to the best of our knowledge, it has not as yet been performed. Alternatively, because of the wide range of the magnitudes of the electric current and different compositions of the alloys, the development of a general theoretical approach to the problem is quite topical.

In this study we investigate the change of the temperature distribution in the bulk of a heterogeneous conductor caused by electric current. The effect of the electric current on the conductor essentially depends on the experimental conditions and a number of parameters: geometry (the width of the conductor, the distance between the inclusion and the conductor's surface, and the size of the inclusion); ratios of thermal and electric conductivity; specific heat and density; and the temperature regime which is maintained at the conductor's surface. All of these dependencies are investigated in the present study.

The presence of particulate inclusions in the conductor is manifested through two mechanisms. The first one is associated with the thermal conductivity jump at the particle's surface while the second one is related to the change of the distribution of the electric current in the conductor in response to the difference in electric conductivities of the particle and the host medium. These two mechanisms manifest themselves differently. The first one has an appreciable effect on the behavior of a system only when the thermal conductivity of the particle is much larger than thermal conductivity of the host medium. In the opposite case, when the thermal conductivity of the inclusion is close to or less than the thermal conductivity of the host medium, the effect of the inclusion on the temperature distribution is insignificant. When the effect of the thermal conductivity jump is significant, the temperature at the location of an inclusion can be significantly higher than the temperature at the same location

a)Authors to whom correspondence should be addressed. Electronic addresses: yuli@bgu.ac.il and elperin@bgu.ac.il.

without an inclusion. The effect of the change of the distribution of electric current in the presence of an inclusion is more involved. In a wide range of parameters, the change of the electric current distribution causes cooling of the heterogeneous conductor in comparison with the homogeneous conductor. In this case, if the surface temperature of the conductor is kept constant, the effect of cooling is always smaller than the effect of heating caused by the first mechanism. Hence the overall effect of an inclusion when the surface temperature of the conductor is kept constant amounts to heating. A special feature of the Joule heating mechanism is that due to the nonlinearity a point symmetry appears in the temperature field. In other words, because of the quadratic dependence of the Joule heating rate on the electric current density, the electric field (having dipole symmetry) induces an isotropic component of the temperature field. This temperature component decays as the inverse distance from the heat source. Due to this low decay rate, the formal space averaging of this component yields divergent integrals and causes certain problems in determining various parameters, e.g., average temperature. Therefore because of the slow (Coulomb type) attenuation of these fields it is necessary to take into account the finite size of the system. The goal of this study is to determine the temperature distribution in a heterogeneous system with internal heat sources for different regimes of heat exchange with the surrounding medium and taking into account the finite size of the system.

In Sec. II we present a mathematical model and determine the temperature distribution when the surface temperature of the conductor is kept constant, neglecting the Joule heating contribution to a heat source caused by the change in the distribution of the electric current. Consequently, in Sec. II we describe the case where electric conductivities of the inclusion and the conductor are equal. In Sec. III we determine the temperature distribution caused by the change in the distribution of the electric current and determine the general behavior of the temperature distribution when the surface temperature of the conductor is kept constant in time. In Sec. IV we determine the temperature distribution in the case of a thermally insulated conductor without heat exchange with the surrounding medium. It is demonstrated that under these circumstances it is feasible to attain substantial cooling of the inclusion with respect to the bulk of the conductor. In the Sec. V we discuss various features of material structural changes in the conductor pertinent to the above-discussed experiments.

II. MATHEMATICAL MODEL AND TEMPERATURE DISTRIBUTION

Consider a solid metal slab with a width d and infinite in y and x directions. At the distance s from the surface of the slab there is a spherical inclusion with a radius a. The parameters of the spherical particle are denoted with the subscript 1 while the parameters of the host medium are denoted by the subscript 2 (see Fig. 1). The density of the electric current far away from the particle does not depend upon these coordinates and equals $\vec{j}_0$. The electric current far away from

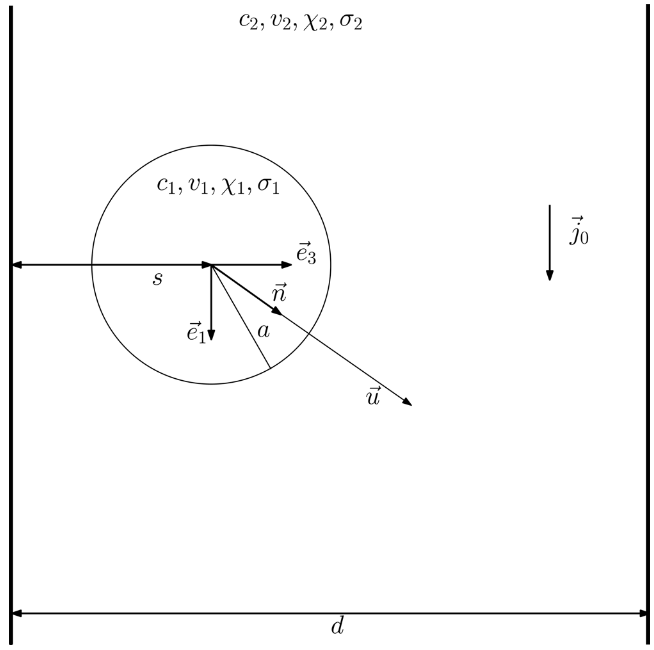

FIG. 1. Schematic view of a slab and the spherical inclusion.

the inclusion is directed along the surface of a slab, $\vec{e}_1$. The temperature distribution in the slab reads:

$$T(\vec{r}, t) = T_1\theta_1 + T_2\theta_2, \tag{1}$$

where $\theta_1 = 1$ inside the inclusion and $\theta_1 = 0$ outside the inclusion, $\theta_2 = 1 - \theta_1$ and T_i is determined by a heat conduction equation with a heat source:

$$\frac{\partial T_i}{\partial t} = \chi_i \vec{\nabla}^2 T_i + \frac{Q_i v_i}{c_i}, \tag{2}$$

where $\vec{\nabla}^2$ is the Laplace operator, χ_i, c_i, v_i are temperature diffusivity, specific heat, and specific volume, respectively, $i = 1, 2.$, $Q_i = \left(\vec{j}_i \cdot \vec{E}_i\right)$, $\vec{j}_i$, $\vec{E}_i$ are the electric current density and the electric field strength in the domain i, and $\vec{E}_i = \vec{j}_i/\sigma_i$, where σ_i is the electrical conductivity in the domain i. Hereafter we neglect the dependence of the kinetic coefficients on temperature. In formulating the boundary conditions for Eq. (2) we assume that the surface temperature of the slab $\overline{T}_0$ is kept constant. Then the boundary conditions at the surface of the inclusion read:

$$T_1 = T_2, \quad \vec{n} \cdot \left(\chi_1 \vec{\nabla} T_1 - \chi_2 \vec{\nabla} T_2\right) = 0, \tag{3}$$

where $\vec{n}$ is a unit vector, $\vec{n} = (\vec{r} - s\vec{e}_3)/|\vec{r} - s\vec{e}_3|$.

The boundary condition at the surface of a slab $z = 0$, $z = d$ is as follows:

$$T_2 = \overline{T}_0. \tag{4}$$

The initial condition for Eq. (2) is $T(\vec{r}, 0) = \overline{T}_0$.

If the heat source Q does not depend on time, the general solution of Eq. (2) can be written as follows: $T(\vec{r}, t) = T_t(\vec{r}, t) + T_s(\vec{r})$, where $T_s(\vec{r})$ is a stationary temperature distribution in the system at $t \rightarrow \infty$ that satisfies the following equation:

$$\chi_i \vec{\nabla}^2 T_i + \frac{Q_i v_i}{c_i} = 0. \tag{5}$$

The term $T_t(\vec{r}, t)$ describes a transient process and it is the solution of Eq. (2) without external heat sources,

$$T_t(\vec{r}, t) = \sum c_n \exp(-\gamma_n t) \phi_n(\vec{r}), \tag{6}$$

where $\phi_n(\vec{r})$ and γ_n is a complete set of eigenfunctions and eigenvalues of Eq. (2) without a heat source which are determined by the boundary conditions given by Eqs. (3) and (4), and the coefficients c_n are determined by the following relation: $c_n = \int \phi_n(\vec{r}) T_t(\vec{r}, 0) d^3\vec{r}$. The initial condition for the temperature distribution yields the initial condition for the function determined by Eq. (6), $T_t(\vec{r}, 0) = \overline{T}_0 - T_s(\vec{r})$. Consequently, if $T_s(\vec{r})$ is known, the problem reduces to determining the eigenfunctions and performing the summation of the series in Eq. (6).

Hereafter we consider only the stationary solution $T = T_s(\vec{r})$ and investigate the behavior of the system in the limit $t \gg d^2/\chi_i$. The stationary temperature distribution $T_s(\vec{r})$ can be written as follows:

$$T_s(\vec{r}) = T_d^0(\vec{r}) + T_d(\vec{r}) + T_a(\vec{r}), \tag{7}$$

where $T_d^0(\vec{r})$ is the temperature distribution in a homogeneous slab with a width d carrying electric current density $\vec{j}_0$ when the temperatures $T_d^0(x, y, 0)$ and $T_d^0(x, y, d)$ at the boundaries $z = 0$, $z = d$ are equal $\overline{T}_0$. Using Eqs. (2) and these boundary conditions, it can be easily found that

$$T_d^0(z) = \overline{T}_0 - \frac{Q_0 v_2}{c_2 \chi_2}\left(z^2 - zd\right), \qquad Q_0 = \frac{j_0^2}{\sigma_2}. \tag{8}$$

The term $T_d(\vec{r})$ in Eq. (7) describes the change of the temperature distribution caused by the presence of the inclusion without taking into account the redistribution of the electric current. The term $T_a(\vec{r})$ in Eq. (7) accounts for the redistribution of the electric current, and consequently the redistribution of the heat source. Each of these terms can be written in the form given by Eq. (1). The function $T_s(\vec{r}) - T_d^0(\vec{r})$ satisfies the following equation:

$$\vec{\nabla}^2\left(T_{si} - T_d^0\right) + Q_i v_i / c_i \chi_i - Q_0 v_2 / c_2 \chi_2 = 0.$$

The above analysis implies that functions $T_{ai}(\vec{r})$ satisfy the following equation:

$$\vec{\nabla}^2 T_{ai} + \frac{Q_0 v_2}{\chi_2 c_2}(\alpha_i Q_{ai} - 1) = 0, \ \alpha_i = \frac{c_2 \chi_2 v_i}{c_i \chi_i v_2}, \ Q_{ai} = \frac{\vec{j}_i \cdot \vec{E}_i}{Q_0}. \tag{9}$$

The boundary conditions are as follows: at the surface of the spherical inclusion, $|\vec{r} - s\vec{e}_3| = a$, $T_{a1} = T_{a2}$, $\vec{n} \cdot \left(\chi_1 \vec{\nabla} T_{a1} - \chi_2 \vec{\nabla} T_{a2}\right) = 0$ and at the surface of a slab $T_{a2} = 0$. Since the function T_{ai} accounts for the effect of the renormalized heat source according to Eq. (9), the function T_{di} is a solution of the heat conduction equation without external heat sources. Therefore the function $T_{di}(\vec{r})$ satisfies the Laplace equation:

$$\vec{\nabla}^2 T_{di} = 0. \tag{10}$$

The boundary conditions for Eq. (10) are as follows: at the surface of a spherical inclusion

$$T_{d1} = T_{d2}, \ \vec{n} \cdot \left(\chi_1 \vec{\nabla} T_{d1} - \chi_2 \vec{\nabla} T_{d2}\right) = (\chi_2 - \chi_1) \vec{n} \cdot \nabla T_d^0, \tag{11}$$

and at the surface of a slab $T_{d2} = 0$. In order to determine the functions $T_{ai}(\vec{r})$ it is necessary to find the renormalized heat sources, Q_{ai}. The latter problem will be solved in Sec. III below. First let us determine the temperature distribution $T_{di}(\vec{r})$ in Eq. (11) which is caused by the gradient of the temperature T_d^0.

We solve the problem with the method of reflections[11] using successive reflections. Herewith, at every stage, one of the boundary conditions that was violated at the previous stage in order to meet another boundary condition is satisfied. The magnitude of the violation of the boundary condition at each stage is proportional to the power of a small parameter. This method allows us to determine a solution in the form of a series of small parameters which in our case are: a/s, a/d, and s/d. The expression for the function $T_{di}(\vec{r})$ can be written as follows:

$$T_{di} = \sum_n T_{di}^{(n)} + \sum_n T_{Rd}^{(n)}, \tag{12}$$

where n is a number of iteration, and the temperature components $T_{di}^{(n)}$ and $T_{Rd}^{(n)}$ are introduced in order to satisfy the boundary conditions at the surface of the inclusion and at the surface of the slab, as required in the method of successive reflections [see Eqs. (13)–(15) below].

Each term in Eq. (12) satisfies the Laplace equation (10) and the corresponding boundary conditions.

At the surface of a spherical inclusion for $n = 0$:

$$T_{d1}^{(0)} = T_{d2}^{(0)}, \quad \vec{n} \cdot \left(\chi_1 \vec{\nabla} T_{d1}^{(0)} - \chi_2 \vec{\nabla} T_{d2}^{(0)}\right) = (\chi_2 - \chi_1) \vec{n} \cdot \vec{\nabla} T_d^0, \tag{13}$$

and for $n \geq 1$,

$$T_{d1}^{(n)} = T_{d2}^{(n)}, \quad \vec{n} \cdot \left(\chi_1 \vec{\nabla} T_{d1}^{(n)} - \chi_2 \vec{\nabla} T_{d2}^{(n)}\right) = (\chi_2 - \chi_1) \vec{n} \cdot \vec{\nabla} T_{Rd}^{(n-1)}. \tag{14}$$

At the surface of the slab

$$T_{d2}^{(n)} + T_{Rd}^{(n)} = 0. \tag{15}$$

In order to solve the problem let us rewrite Eq. (8) in spherical coordinates with the origin at the center of the inclusion using Legendre polynomials, $P_\ell(u)$, where $P_2(\mu) = (3\mu^2 - 1)/2$, $P_1(\mu) = \mu$, and $P_0(\mu) = 1$. Then

$$T_d^0 = \overline{T}_0 - T_j\left(\frac{s(s-d)}{a^2} + \frac{u^2}{3} + \frac{2u^2}{3} P_2(\mu) + \mu\, u \frac{2s - d}{a}\right), \tag{16}$$

where $u = |\vec{r} - s\vec{e}_3|/a$, and $\mu = (\vec{n} \cdot e_3)$. The parameter T_j is determined by the following formula:

$$T_j = \frac{Q_0 a^2 v_2}{c_2 \chi_2}. \quad (17)$$

The parameter T_j characterizes the Joule heat per unit mass of the host conductor with a given heat capacity which is released during time a^2/χ_2. The functions $T_d^{(n)}/T_j$ can be also expanded in the Legendre polynomials, $P_\ell(\mu)$, series:

$$T_{di}^{(n)} = T_j \sum_{\ell=0,1,2} T_{di}^{(n)\ell}(u) P_\ell(\mu). \quad (18)$$

The boundary condition [Eq. (13)] for $T_{di}^{(0)\ell}(u)$ yields (for $\ell = 0$):

$$T_{d1}^{(0)0} = \frac{2(\chi - 1)}{3}, \quad T_{d2}^{(0)0} = \frac{2(\chi - 1)}{3u}, \quad \chi = \frac{\chi_1}{\chi_2}. \quad (19)$$

The functions $T_{d1}^{(0)0}$ and $T_{d2}^{(0)0}$ describe an isotropic temperature distribution component with respect to the center of the inclusion. This component arises due to the following two reasons: (i) the presence of the isotropic component in the initial temperature T_d^0 [the second term in the parentheses in Eq. (16)], and (ii) different thermal conductivities of the inclusion and the host conductor. Depending on the magnitude of the parameter χ this component can be positive or negative which results in additional heating or cooling. Formulas for the dipole component read:

$$T_{d1}^{(0)1} = \frac{(\chi - 1)}{a(\chi + 2)}(2s - d)u, \quad T_{d2}^{(0)1} = \frac{(\chi - 1)}{a(\chi + 2)u^2}(2s - d) \quad \text{for } \ell = 1. \quad (20)$$

Equation (20) describes the dependence of the dipole component (with respect to the inclusion center) of the temperature field versus the distance from the inclusion center u. In contrast with the isotropic component given by Eq. (19), the dipole component depends upon the thickness of the conductor, d. The contribution of this component for a given density of the electric current j_0 grows when this parameter increases. Note that the terms given by Eq. (20) change their signs at $s = d/2$. However, according to Eq. (18) the final contribution of this component is determined by the coefficient $P_1(\mu) = \mu$. Since for $s < d/2$, $\mu = -1$, and $\mu = 1$ for $s > d/2$, the resulting temperature field with a dipole symmetry does not change sign at $s = d/2$ and the sign is determined by the magnitude of the parameter χ as is the case for the isotropic component. The expression for the quadrupole component which is multiplied by coefficient $P_2(\mu)$ reads:

$$T_{d1}^{(0)2} = \frac{4(\chi - 1)}{2\chi + 3} u^2 \; T_{d2}^{(0)2} = \frac{4(\chi - 1)}{(2\chi + 3)u^3} \quad \text{for } \ell = 2. \quad (21)$$

Since the temperature at the boundaries of the conductor, $z = 0$, $z = d$, is kept constant, there occurs an additional contribution to the temperature field. This contribution is associated with the boundary conditions in Eq. (15) and is described by the temperature component, T_{Rd}.

In the first approximation, $T_{Rd} = T_{Rd}^{(0)}$, where the expression for $T_{Rd}^{(0)}$ can be written as follows:

$$T_{Rd}^{(0)} = T_j\left(T_{Rd}^{(0)0} + T_{Rd}^{(0)1} + T_{Rd}^{(0)2}\right), \quad (22)$$

and the functions $T_{Rd}^{(0)\ell}$ satisfy the following boundary conditions:

$$T_{Rd}^{(0)\ell} + T_{d2}^{(0)\ell} P_\ell(\mu) = 0 \text{ at } z = 0,\ d. \quad (23)$$

Equation (23) determines the temperature component $T_{Rd}^{(0)\ell}$. Therefore the boundary condition at the surface of the slab determines for each component ℓ of the multipole expansion at the surface of the inclusion, the temperature component, $T_{Rd}^{(0)\ell}$.

For further analysis it is convenient to introduce functions $u_N = |\vec{r} - (2dN + s)\vec{e}_3|/a$ and $u_N^+ = |\vec{r} + (2dN + s)\vec{e}_3|/a$, where N is an integer. These functions satisfy the following relations: for $z = 0$, $u_N = u_N^+$ and for $z = d$, $u_{N+1} = u_N^+$. Using these relations, Eq. (15), and Eq. (23) for $\ell = 0$ we find that

$$T_{Rd}^{(0)0} = \frac{2(\chi - 1)}{3}\left(\sum_{N\neq 0,-\infty}^{\infty} \frac{1}{u_N} - \sum_{-\infty}^{\infty} \frac{1}{u_N^+}\right). \quad (24)$$

Now let us introduce functions, $\mu_N = (\vec{u}_N \cdot \vec{e}_3)/u_N$ and $\mu_N^+ = (\vec{u}_N^+ \cdot \vec{e}_3)/u_N^+$, where vectors $\vec{u}_N$, $\vec{u}_N^+$ have the corresponding absolute values u_N, u_N^+. Clearly, at $z = 0$, $\mu_N = -\mu_N^+$, and at $z = d$, $\mu_{N+1} = -\mu_N^+$. The latter relations and Eq. (15) yield formulas for $T_{Rd}^{(0)\ell}$:

$$T_{Rd}^{(0)1} = \frac{(\chi - 1)}{a(\chi + 2)}(2s - d)\left(\sum_{N=-\infty}^{\infty} \frac{\mu_N^+}{(u_N^+)^2} + \sum_{N\neq 0,-\infty}^{\infty} \frac{\mu_N}{(u_N)^2}\right), \quad (25)$$

$$T_{Rd}^{(0)2} = \frac{4(\chi - 1)}{2\chi + 3}\left(\sum_{N\neq 0,-\infty}^{\infty} \frac{P_2(\mu_N)}{(u_N)^3} - \sum_{N=-\infty}^{\infty} \frac{P_2(\mu_N^+)}{(u_N^+)^3}\right). \quad (26)$$

In order to use the boundary condition (14) for determining the next correction, $T_{di}^{(1)} = T_j \sum_{\ell=0,1,2} T_{di}^{(1)\ell}(u) P_\ell(\mu)$, it is convenient to write the functions given by Eqs. (23)–(25) in the system of coordinates with the origin at the center of the spherical inclusion. To accomplish this we use the transformation which relates the solutions of the Laplace equation $P_k(\mu_N)/(u_N)^{k+1}$ written in systems of coordinates with different origins (see Ref. 12). For $u < 2d$ this relation reads:

$$\frac{P_k(\mu_N)}{(u_N)^{k+1}} = \frac{(-1)^k}{(2dN)^{k+1}} sign(N) \sum_{m=0}^{\infty} \binom{k+m}{m} \frac{u^m P_m(\mu)}{(2dN)^m},$$

$$\frac{P_k(\mu_N^+)}{(u_N^+)^{k+1}} = \frac{1}{(2dN+2s)^{k+1}} sign(2dN+2s) \sum_{m=0}^{\infty} (-1)^m \binom{k+m}{m} \times \frac{u^m P_m(\mu)}{(2dN+2s)^m}. \quad (27)$$

In order to simplify notations let us introduce the following functions:

$$t_{km}(N) = (-1)^k sign(N) \binom{k+m}{m} \left(\frac{1}{(2dN)^{m+k+1}} + \frac{(-1)^{m+1} sign(2dN+2s)}{(2dN+2s)^{m+k+1} sign(N)} \right),$$
$$\bar{t}_{km}(0) = (-1)^{m+1} \binom{k+m}{m} \frac{1}{(2s)^{m+k+1}}. \quad (28)$$

Using these functions, the expression for the temperature component $T_{Rd}^{(0)}$ can be rewritten using Eq. (22) and Eqs. (24)–(26) as follows:

$$T_{Rd}^{(0)} = \sum_{m=0}^{\infty} \sum_{k=0,1,2} f(k) \left(\sum_{N \neq 0 - \infty}^{\infty} t_{km}(N) + \bar{t}_{km}(0) \right) u^m P_m(\mu), \quad (29)$$

where $f(0) = [2(\chi-1)]/3$, $f(1) = [(\chi-1)(2s-d)]/[a(\chi+2)]$, $f(2) = [4(\chi-1)]/(2\chi+3)$.

Substituting Eq. (29) into the right-hand side of the second expression in Eqs. (14) we arrive at the following correction to the functions T_{di}:

$$T_{d1}^{(1)\ell} = \frac{(1-\chi)t_\ell}{\ell\chi + \ell + 1} u^\ell, \quad T_{d2}^{(1)\ell} = \frac{(1-\chi)t_\ell}{\ell\chi + \ell + 1} \frac{1}{u^{\ell+1}}, \quad (30)$$

where

$$t_\ell = \ell \sum_{k=0,1,2} f(k) \left(\sum_{N \neq 0, -\infty}^{\infty} t_{k\ell}(N) + \bar{t}_{k\ell}(0) \right). \quad (31)$$

The above procedure can be repeated in order to determine the successive terms in the expansion. However there is no need to perform these calculations since the successive terms in the expansion yield small corrections with respect to the characteristic temperature. Consequently, the solution of the problem is as follows:

$$T_{di}(r) = T_j \left[\sum_{\ell=0,1,2} \left(T_{di}^{(0)\ell} + T_{di}^{(1)\ell} \right) P_\ell(\mu) + T_{Rd}^{(0)0} + T_{Rd}^{(0)1} + T_{Rd}^{(0)2} \right].$$

The derived formulas allow us to perform a complete analysis of the temperature distribution, $T_d + T_d^0 = T_s - T_a$. Before presenting the obtained results let us consider the most significant parameters of the problem. First, it must be noted that according to Eq. (8), $T_d^0 \propto z^2$. Since z varies at the scale of the conductor width d, for a given density of the electric current the temperature of the conductor is $T_d^0 \propto T_j d^2/a^2$. At the same time, according to the boundary conditions (13) and (14), the temperature field T_d associated with the inclusion is proportional to $\vec{\nabla} T_d^0$ and, consequently, increases as $\propto T_j\, \chi\, d/a$. Therefore the presence of the inclusion has a significant effect when the parameter $\chi = \chi_1/\chi_2$ is of the order of $\sim d/a$ or larger. In the opposite case, $\chi \leq 1$, the presence of the inclusion does not have a significant effect on the temperature distribution in the conductor (until now we have not taken into account the change of electric current distribution). Conversely, it can be shown using the boundary condition (11) and Eq. (8) that for $\chi > 1$ the presence of the inclusion is equivalent to introducing a surface heat source while for $\chi < 1$ the presence of the inclusion is equivalent to a heat sink. If one assumes that the temperature diffusivity ratio does not depend on the temperature, the inclusion causes heating in the vicinity of the particle which is proportional to the parameter χ, while the magnitude of cooling (in case it occurs) is bounded by a small parameter. In the latter case, $(T_s - T_a)/T_d^0 \sim a/d$. Clearly, these considerations have only an *a priori* character. The Eqs. (19)–(24) and (29)–(30) derived above allow us to perform an extensive analysis that demonstrates that the inclusion strongly affects the temperature field only when the temperature diffusivity of the inclusion is considerably larger than that of the surrounding medium. The effect of the inclusion is associated with the terms $T_{Rd}^{(0)0}$ and $T_{di}^{(0)0}$ which can be strongly changed by varying the magnitude of the parameter χ. Other terms, $T_{di}^{(0)\ell}$ and $T_{Rd}^{(0)\ell}$ $(\ell = 1, 2)$, weakly vary for large values of the parameter χ and tend to their asymptotic values [see Eqs. (20), (21), (23), and (24)].

The azimuthal symmetry of the function $\Delta = T_s(\vec{r}) - T_a(\vec{r})$ allows us to represent it as $\Delta(\vec{r}) = \Delta(z, \rho)$, where ρ is the distance from the axis z passing through the center of the inclusion and perpendicular to the slab surface. In Fig. 2 we show the behavior of the function $D(z, \rho) = \left[\Delta(z, \rho) - \overline{T}_0\right]/T_j$ for different distances s between the center of the inclusion and the left boundary for $\rho = 0$ ($\overline{T}_0$ is the surface temperature of the slab). In Fig. 3 we plot the function $D(z, \rho)$ for different distances ρ from the axis of symmetry when the center of the inclusion is located at the same distance from the left and right boundaries of the conductor, $s = d/2$. All of the length parameters d, s, ρ are measured in units of the particle radius, $a = 1$. The spatial temperature dependence $D(\vec{r}) = D(z, \rho)$ exhibits a mirror symmetry, i.e., temperature distribution caused by the inclusion with the center at s is related to the temperature distribution caused by the inclusion with the center at $d - s$ by the mirror reflection transformation with respect to a plane $z = d/2$. Due to these circumstances we plotted temperature distributions only for the cases which are not related by the mirror reflection transformation (see Fig. 2). The maximum temperature difference between the inhomogeneous and homogeneous conductors D is attained at $z = d/2$. Inspection

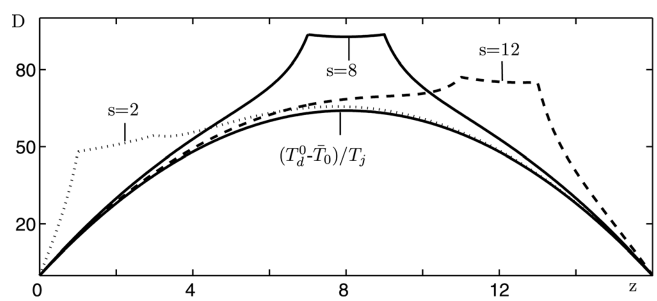

FIG. 2. Dependence of $D = (\Delta - \bar{T}_0)/T_j$ vs distance z from the left surface of the slab, $z = 0$, for different distances s between the center of the spherical inclusion and the left surface of the slab. The distance from the axis of symmetry of the system: $\rho = 0$, $a = 1$, $d = 16$, $\chi = 48$.

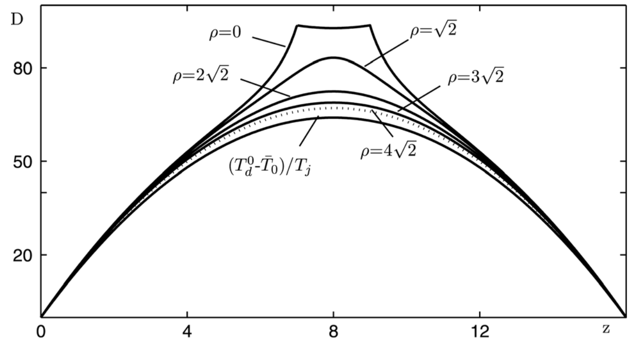

FIG. 3. Dependence of $D=(\Delta-\bar{T}_0)/T_j$ vs distance z from the left surface of the slab, $z=0$, for different distances from the axis of symmetry of the system, ρ. The distance between the center of the spherical inclusion and the left surface of the slab: $s=8$, $a=1$, $d=16$, $\chi=48$.

of Fig. 3 reveals an essential difference between the temperatures in the inhomogeneous and homogeneous slabs only in the vicinity of the axis of symmetry passing through the center of the inclusion and perpendicular to the faces of the slab. The effect of the inclusion rapidly diminishes with distance from the axis. In Figs. 2 and 3 we show the behavior of the temperature field for large magnitudes of the thermal conductivity ratio χ. The above analysis demonstrates that when this parameter decreases the effect of the inclusion diminishes. Now let us determine the functions $T_{ai}(\vec{r})$.

III. EFFECT OF CHANGE OF THE DISTRIBUTION OF ELECTRIC CURRENT ON JOULE HEATING OF INCLUSIONS

In order to determine functions T_{ai} we again use the method of reflections[10] whereby functions T_{ai} are represented as follows:

$$T_{ai}=\sum_n T_{ai}^{(n)}+\sum_n T_{Ra}^{(n)}. \tag{32}$$

At the surface of the spherical inclusion, $|\vec{r}-s\vec{e}_3|=a$, $T_{a1}=T_{a2}$, $\vec{n}\cdot\left(\chi_1\vec{\nabla}T_{a1}-\chi_2\vec{\nabla}T_{a2}\right)=0$ and at the slab's surface $T_{a2}=0$. The functions $T_{ai}^{(0)}$ are determined by Eqs. (9) and satisfy the same boundary conditions at the surface of the inclusion, $|\vec{r}-s\vec{e}_3|=0$, as functions T_{ai}. The functions $T_a^{(n)}$ for $n\geq 1$ are determined by the Laplace equation, $\vec{\nabla}^2 T_{ai}^{(n)}=0$, and satisfy the following boundary conditions at the surface of the spherical inclusion:

$$T_{a1}^{(n)}=T_{a2}^{(n)},\ \vec{n}\cdot\left(\chi_1\vec{\nabla}T_{a1}^{(n)}-\chi_2\nabla T_{a2}^{(n)}\right)=(\chi_2-\chi_1)\vec{n}\cdot\vec{\nabla}T_{Ra}^{(n-1)}. \tag{33}$$

The functions $T_{Ra}^{(n)}$ are determined by the Laplace equation:

$$\vec{\nabla}^2 T_{Ra}^{(n)}=0,\ T_{a2}^{(n)}+T_{Ra}^{(n)}=0\ \text{at}\ z=0,\ z=d. \tag{34}$$

Therefore in order to find the temperature distribution, $T_a(\vec{r})$, it is first necessary to determine the heat sources Q_{ai}. In the magnetostatic approximation (for details, see Ref. 7), the distribution of electric current is determined by the following equations:

$$\vec{\nabla}\cdot\vec{j}=0,\quad \vec{\nabla}\times\vec{E}=0,\quad \vec{j}=\sigma\vec{E}.$$

The formula for the electric current density reads:

$$\begin{aligned}&\vec{j}=\vec{j}_1\theta_1+\vec{j}_2\theta_2,\quad \vec{j}_1=\vec{j}_0\frac{3\kappa}{\kappa+2},\\&\vec{j}_2=\vec{j}_0\left[1-2\xi\frac{a^3}{r^3}P_2^0(\vec{n}\cdot\vec{e}_1)\right]-\xi\,\vec{e}_\perp j_0\frac{a^3}{r^3}P_2^1,\end{aligned} \tag{35}$$

where $\xi=(1-\kappa)/(\kappa+2)$, $\kappa=\sigma_1/\sigma_2$, $\cos\vartheta_1=\vec{n}\cdot\vec{e}_1$, $P_2^1=3\sin\vartheta_1\cos\vartheta_1$, and $\vec{e}_\perp$ is a unit vector perpendicular to the direction of the electric current $\vec{e}_1$.

Expression (35) is obtained in the approximation of an infinite medium. In the case of a slab the electric current density must satisfy the additional condition, namely, the vanishing of the normal component of the electric current density at the slab's surface. The latter condition changes only the last term in Eq. (35) which is proportional to $\vec{e}_\perp$. All calculations hereafter are performed using Eq. (35) with the accuracy of the terms of the order of a^3/s^3. The above formulas yield:

$$\alpha Q_{a1}-1=\frac{9\alpha\kappa}{(\kappa+2)^2}-1, \tag{36}$$

where $\alpha=\alpha_1$ [$\alpha_2=1$, see Eq. (9)].

Formulas (9) and (36) imply that a heat source (36) is a heat sink when $\alpha<8/9$. The maximum cooling rate is attained for large $\kappa\gg\max\{1,\alpha\}$ and infinitely small values of κ, i.e., $\alpha\kappa\ll 1$. In these limiting cases $\alpha Q_{a1}-1=-1$. The minimum cooling rate is attained for $\kappa=2$ where $\alpha Q_{a1}-1=9\alpha/8-1$. When $\alpha>8/9$ in the interval of the electric conductivity, $\kappa_2<\kappa<\kappa_1$; where $\kappa_{1,2}=1/2\big(9\alpha-4\pm 9\sqrt{(\alpha-8/9)\alpha}\big)$, the inclusion acts as an additional heat source. In contrast to the case of a heat sink the heating rate grows infinitely with the increase of the ratio of thermal conductivities, α.

The above formulas yield an expression for a heat source, Q_{a2} in the form of a Legendre polynomials series:

$$Q_{a2}-1=u^{-6}\xi^2(2P_2(\cos\vartheta_1)+2)-4u^{-3}\xi P_2(\cos\vartheta_1). \tag{37}$$

Formula (9) indicates the reason for neglecting the contribution from the additional term in the expression for the electric current density that corresponds to the reflection of the electric current density term $\propto e_\perp$ as mentioned above. Indeed, it is easily seen that the contribution of this term in the heat source is of the order of a^6/s^6.

Now let us introduce a function Q_i^ℓ, where $Q_1^0=-(\alpha Q_{a1}-1)$ is determined by Eq. (36), and $Q_2^0=-2\xi^2/u^6$, $Q_2^2=(-2/u^6)\xi^2+(4/u^3)\xi$. The expression for the functions $T_{ai}^{(0)}$ can be written as follows:

$$\frac{T_{ai}^{(0)}}{T_j}=\sum_{0,2}T_{ai}^{(0)\ell}(u)P_\ell(\cos\vartheta_1). \tag{38}$$

The dimensionless temperatures, $T_{ai}^{(0)\ell}$, $\ell=0,\ 2$, are determined by the following equation:

$$\frac{\partial^2 T_{ai}^{(0)\ell}}{\partial u^2}+\frac{2}{u}\frac{\partial T_{ai}^{(0)\ell}}{\partial u}-\frac{\ell(\ell+1)}{u^2}=Q_i^\ell. \tag{39}$$

Solutions of these equations with corresponding boundary conditions at the surface of the inclusion read:

$$T_{a1}^{(0)0} = \frac{\xi^2}{2} - \frac{2\chi+1}{6}Q_1^0 + \frac{Q_1^0}{6}u^2,\; T_{a2}^{(0)0} = \left(\frac{2}{3}\xi^2 - \frac{\chi Q_1^0}{3}\right)\frac{1}{u} - \frac{\xi^2}{6u^4}, \tag{40}$$

$$\begin{aligned} T_{a1}^{(0)2} &= -\frac{\xi^2+4\xi}{3(3+2\chi)}u^2, \\ T_{a2}^{(0)2} &= \frac{1}{3u^3}\frac{2\xi(2\chi+1)-(2\chi+4)\xi^2}{(3+2\chi)} + \frac{\xi^2}{3u^4} - \frac{2\xi}{3u}. \end{aligned} \tag{41}$$

In order to derive expressions for the functions $T_{Ra}^{(0)}$ given by Eq. (34) it is sufficient to keep only the terms of the order of $\sim 1/u$ since the rest of the terms are of the order of a^3/s^3, a^3/d^3 and higher at the surface of a slab. Consequently, the corresponding compensating corrections can be neglected without violating the initially chosen accuracy of the calculations. The procedure for determining the function $T_{Ra}^{(0)0}$ is absolutely similar to the procedure for calculating the function $T_d^{(0)0}$. The final result is as follows:

$$T_{Ra}^{(0)0} = \left(\frac{2\xi^2}{3} - \frac{\chi Q_1^0}{3}\right)\left[\frac{1}{u_0^+} - \sum_{N\neq 0,-\infty}^{\infty}\left(\frac{1}{u_N} - \frac{1}{u_N^+}\right)\right].$$

Repeating the procedure used above for calculating T_d, we arrive at the following formulas for T_{ai}:

$$\frac{T_{ai}}{T_j} = \sum_{\ell=0,2} T_{ai}^{(0)\ell}(u)P_\ell(\vec{n}\cdot\vec{e}_1) + T_{Ra}^{(0)0} + \sum_{\ell=0}^{\infty} T_{ai}^{(1)\ell}(u)P_\ell(\mu), \tag{42}$$

where

$$\begin{aligned} T_{a1}^{(1)\ell} &= \frac{(1-\chi)t_{a\ell}}{\ell\chi+\ell+1}u^\ell,\; T_{a2}^{(1)\ell} = \frac{(1-\chi)t_{a\ell}}{\ell\chi+\ell+1}\frac{1}{u^{\ell+1}}, \\ t_{a\ell} &= \ell\left(\frac{2}{3}\xi^2 - \frac{\chi Q_{10}}{3}\right)\sum_{N\neq 0,-\infty}^{\infty} t_{0\ell}(N) + \bar{t}_{0\ell}(0), \end{aligned} \tag{43}$$

and $t_{0\ell}(N)$ and $\bar{t}_{0\ell}(0)$ are determined by Eqs. (28).

In Figs. 4 and 5 we plotted the function $T_a(\vec{r})/T_j = (T_{a1}\theta_1 + T_{a2}\theta_2)/T_j$. Inspection of these figures shows that the temperature $T_a(\vec{r})$ can be negative relative to the conductor's surface (see Fig. 4) or positive (see Fig. 5). This effect is caused by the source $Q_1^0 = -(\alpha Q_{a1} - 1)$ which, depending on the parameters identified above, can act either as a heat source or a heat sink. On the other hand, formulas (40) show that when χ increases, the effect of the source Q_1^0 is enhanced since the magnitude of α decreases. The latter readily allows us to attain large negative temperature differences. However, the increase of χ is accompanied by the increase of $\Delta = T_s(\vec{r}) - T_a(\vec{r})$, that compensates for the effect of $T_a(\vec{r})$ so that the total effect is the increase of the temperature in comparison with the temperature in a homogeneous conductor T_d^0. The resulting temperature is shown in Figs. 6 and 7 where Fig. 6 corresponds to the case when Q_1^0 is a heat sink and Fig. 7 illustrates the case when Q_1^0 is a heat source. Clearly, in the latter case the magnitude of the heating is considerably larger. The above analysis shows that for cooling the inclusion relative to the conductor surface it is necessary to decrease the term $\Delta = T_d + T_d^0$. Reduction of T_d can be achieved when $\chi = 1$ and consequently, $T_d = 0$. In order to reduce T_d^0 we consider small values of d. Since the diameter of the inclusion $2a = 2$ and for very small values of d/a the accuracy of the calculations declines, we considered the cases with $d = 3$ and $d = 5$. The difference between these two cases is small, and in Fig. 8 we showed only the case when $d = 5$. In order to exclude the

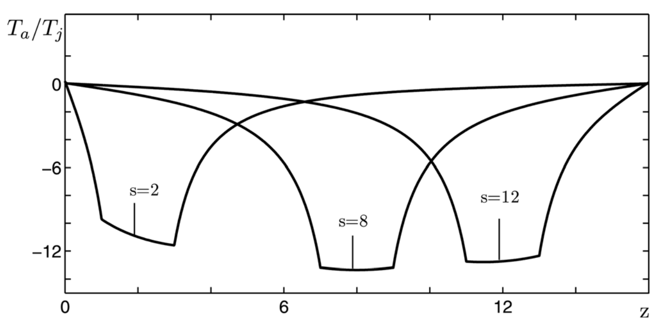

FIG. 4. Dependence of T_a/T_j vs distance z from the left surface of the slab $z = 0$, for different distances s between the center of the spherical inclusion and the left slab surface: $a = 1$, $d = 16$, $\rho = 0$, $\chi = 48$, $\kappa = 33$, $\alpha = 0.3$.

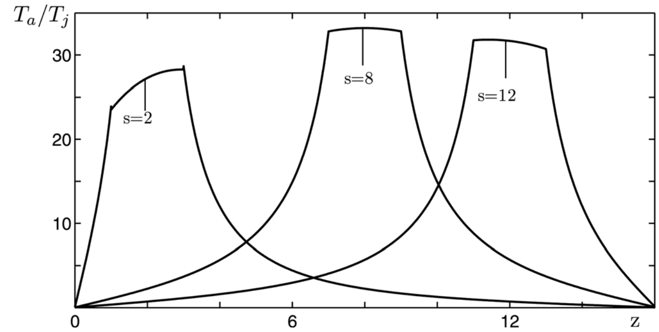

FIG. 5. Dependence of T_a/T_j vs distance z from the left surface of the slab $z = 0$, for different distances s between the center of the spherical inclusion and the left slab surface: $a = 1$, $d = 16$, $\rho = 0$, $\chi = 48$, $\kappa = 3$, $\alpha = 3$.

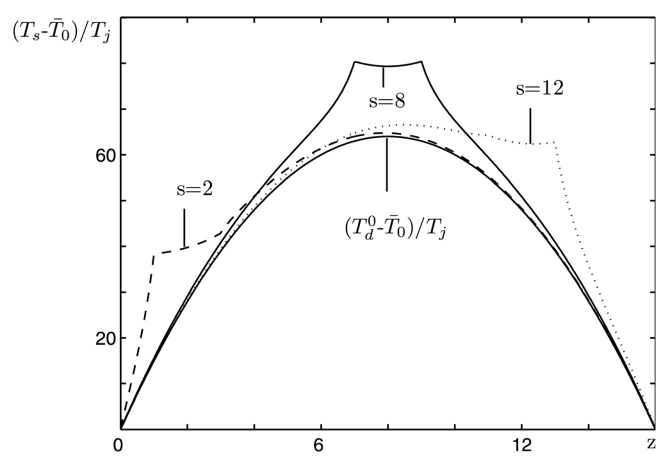

FIG. 6. Dependence $(T_s - \bar{T}_0)/T_j$ vs distance z from the left surface of the slab $z = 0$, for different distances s between the center of the spherical inclusion and the left slab surface for the case when Q_1^0 is a heat sink: $a = 1$, $d = 16$, $\chi = 48$, $\rho = 0$, $\alpha = 0.3$.

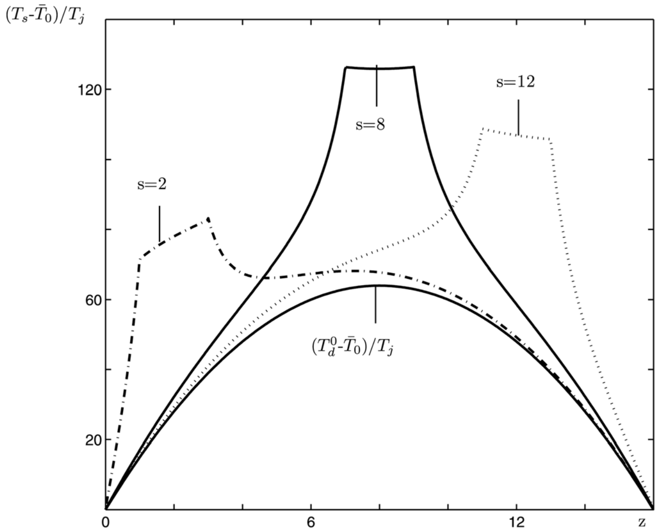

FIG. 7. Dependence $(T_s - \bar{T}_0)/T_j$ vs distance z from the left surface of the slab $z = 0$, for different distances s between the center of the spherical inclusion and the left slab surface for the case when Q_1^0 is a heat source: $a = 1$, $d = 16$, $\chi = 48$, $\rho = 0$, $\alpha = 3$.

effect of thermal diffusivity ratio it is assume that $\chi = 1$. Inspection of this figure demonstrates that in this case the temperature in a heterogeneous conductor with an inclusion is only slightly different from the temperature in the homogeneous conductor, T_d^0.

Therefore the temperature inside the conductor cannot be smaller than its surface temperature during stationary heating of a conductor by electric current. The reason is that even when the contribution of T_d is eliminated by assuming $\chi = 1$, the contribution of T_d^0 is always larger than the absolute value of the cooling. It must be noted that the magnitude of the cooling shown in Fig. 5 is obtained for a large magnitude of the temperature diffusivity ratio, χ. Decreasing the thermal diffusivity ratio causes the decrease of not only the temperature component T_d but also the decrease of the temperature component T_a which is caused by the change of distribution of the electric current. The latter assertion follows from the expression for the second term in the formula for the function $T_{a1}^{(0)0}$ [see Eq. (40) for $\chi = 1$] and the second term in Eq. (40) for the function $T_{a2}^{(0)0}$.

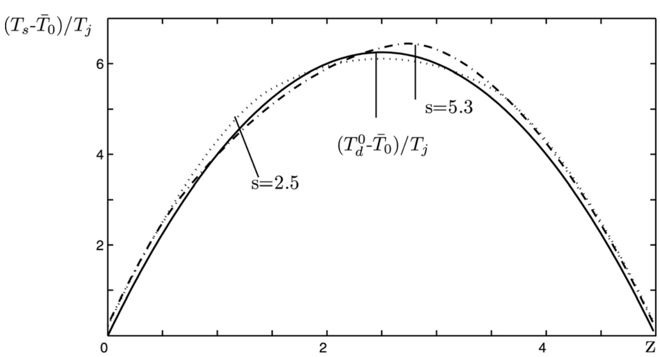

FIG. 8. Dependence $(T_s - \bar{T}_0)/T_j$ vs distance z from the left surface of the slab $z = 0$, for different distances s between the center of the spherical inclusion and the left slab surface when the size of the inclusion is close to the width of the slab: $a = 1$, $d = 5$, $\rho = 0$, $\chi = 1$, $\kappa = 33$, $\alpha = 0.01$.

The temperature in a homogeneous conductor is expressed as $T_d^0 \propto (d^2/4a^2)T_j$, and since $d > 2a$, T_d^0 is always larger than the magnitude of cooling which is less than $T_j/3$ [see the second term in Eq. (40) for $\chi = 1$]. Consequently, the slab is always heated relative to its surface when the surface temperature is kept constant.

We consider the case when both faces of the slab are maintained at the same temperature, $\overline{T}_0$. Analysis of a more general case when the temperatures of the two faces of a slab, $z = 0$ and $z = d$, are different and equal $\overline{T}_0$ and $\overline{T}_d$, reduces to the appearance of the additional term in Eq. (8):

$$T_d^0 = \overline{T}_0 - \frac{Q_0 v_2}{c_2 \chi_2}\left(z^2 - zd\right) + \left(\overline{T}_d - \overline{T}_0\right)\frac{zd}{d^2}.$$

This transformation is equivalent to imposing the additional constant temperature gradient $\left(\overline{T}_d - \overline{T}_0\right)/d$. In order recover this case in the derived formulas it is sufficient to replace the coefficient $(2s - d)/d$ by $(2s - d)/d + \left(\overline{T}_d - \overline{T}_0\right)a^2/d^2T_j$ in all formulas. The latter transformation only violates symmetry with respect to the plane $z = d/2$. It must be noted that if $\left(\overline{T}_d - \overline{T}_0\right)/T_j > d^2/(2a^2)$ then the temperature distribution in a homogeneous slab is monotone.

IV. TEMPERATURE DISTRIBUTION IN THE HETEROGENEOUS AND THERMALLY INSULATED CONDUCTOR

So far it has been assumed that the surface temperature of the conductor is kept constant. In practice this situation occurs in the presence of surface endothermic processes, e.g., the evaporation of liquid having a large latent heat of phase transition. If the thermal conductivity of the surrounding medium is significantly smaller than the thermal conductivity of the conductor and radiative heat transfer is negligibly small, the system can be considered thermally insulated. The boundary condition in this case is $\vec{\nabla} T_2 = 0$. Let us determine the temperature distribution in this system. In the homogeneous conductor the only solution that satisfies the above boundary condition reads:

$$T_2(t) = \frac{Q_0 v_2}{c_2} t. \tag{44}$$

This solution describes the heating of a homogeneous thermally insulated slab whereby the temperature increases with time. The stationary solution in a thermally insulated system with a heat source does not exist. In the presence of the spherical inclusion the temperature distribution is inhomogeneous, and we seek the solution in the following form:

$$T(\vec{r}, t) = T_b(\vec{r}, t) + T_2(t). \tag{45}$$

Formulas (44) and (45) yield the following equation for $T_{bi}(\vec{r}, t)$:

$$\frac{\partial T_{bi}}{\partial t} = \chi_i \vec{\nabla}^2 T_{bi} + \frac{Q_0 v_2}{c_2}(\beta_i Q_{ai} - 1), \quad \beta_i = \frac{c_2 v_i}{v_2 c_i}, \tag{46}$$

where Q_{ai} is determined by Eq. (9). A general solution of Eq. (46) can be represented in a similar manner to the general solution of Eq. (2) as $T_b(\vec{r},t) = T_t(\vec{r},t) + T_{bs}(\vec{r})$. Equation (44) implies that $T_2(0) = 0$, and consequently, we obtain the following initial condition:

$$T_t(0) = \overline{T}_0 - T_{bs}(\vec{r}),$$

where $T_{bs}(\vec{r})$ is the solution of a stationary problem and $\overline{T}_0$ is the initial temperature.

Similarly to the previous sections our goal is to determine the stationary component, $T_{bs}(\vec{r})$. When $t \gg d^2/\chi_i$, the temperature distribution is $T(\vec{r},t) = T_{bs}(\vec{r}) + T_2(t)$. The equation for the stationary component of temperature, T_b, reads:

$$\bar{\chi}_i \vec{\nabla}^2 T_{bi} + \frac{T_j}{a^2}(\beta_i Q_{ai} - 1) = 0, \quad \bar{\chi}_i = \chi_i/\chi_2.$$

Functions T_{bi} can be exactly calculated in the same manner as functions T_{ai}. The only difference is that at the slab surface instead of the boundary condition (34) we have $\vec{e}_3 \cdot \vec{\nabla}\left(T_{b2}^{(n)} + T_{Rb}^{(n)}\right) = 0$. The final solution of the problem reads:

$$T_{bi}/T_j = \sum_{l=0,2} T_{bi}^{(0)l}(u)P_l(\vec{n}\cdot\vec{e}_1) + T_{Rb}^{(0)0} + \sum_{l=0}^{\infty} T_{bi}^{(1)l}(u)P_l(\mu),$$

where

$$\begin{aligned} T_{b1}^{(0)0} &= \frac{\xi^2}{2} - \frac{2\chi+1}{6}\bar{Q}_1^0 + \frac{\bar{Q}_1^0}{6}u^2, \\ T_{b2}^{(0)0} &= \left(\frac{2}{3}\xi^2 - \frac{\chi\bar{Q}_1^0}{3}\right)\frac{1}{u} - \frac{\xi^2}{6u^4}, \\ T_{b1}^{(0)2} &= -\frac{\xi^2+4\xi}{3(3+2\chi)}u^2, \\ T_{b2}^{(0)2} &= \frac{1}{3u^3}\frac{2\xi(2\chi+1)-(2\chi+4)\xi^2}{(3+2\chi)} + \frac{\xi^2}{3u^4} - \frac{2\xi}{3u}, \end{aligned} \tag{47}$$

and the terms

$$\bar{Q}_1^0 = -\frac{\beta Q_{a1} - 1}{\chi}, \tag{48}$$

$$T_{Rb}^{(0)0} = \left(\frac{2\xi^2}{3} - \frac{\chi\bar{Q}_1^0}{3}\right)\left[\frac{1}{u_0^+} + \sum_{N\neq 0,-\infty}^{\infty}\left(\frac{1}{u_N} + \frac{1}{u_N^+}\right)\right],$$

$$T_{b1}^{(1)l} = \frac{(1-\chi)t_{b\ell}}{\ell\chi + \ell + 1}u^\ell, \tag{49}$$

$$\begin{aligned} T_{b2}^{(1)\ell} &= \frac{(1-\chi)t_{b\ell}}{\ell\chi+\ell+1}\frac{1}{u^{\ell+1}}, \\ t_{b\ell} &= \ell\left(\frac{2}{3}\xi^2 - \frac{\chi\bar{Q}_{10}}{3}\right)\sum_{N\neq 0,-\infty}^{\infty} t_{0\ell}(N) + \bar{t}_{0\ell}(0), \end{aligned} \tag{50}$$

$t_{0\ell}(N)$ and $\bar{t}_{0\ell}(0)$ are determined by Eqs. (26).

In Figs. 9 and 10 we have shown the temperature distribution along the axis passing through the center of the inclusion and perpendicular to the slab. Equation (48) implies the feasibility of the strong cooling of the inclusion by reducing the temperature diffusivities ratio, χ. When χ is large the inclusion is heated with respect to the conductor's surface

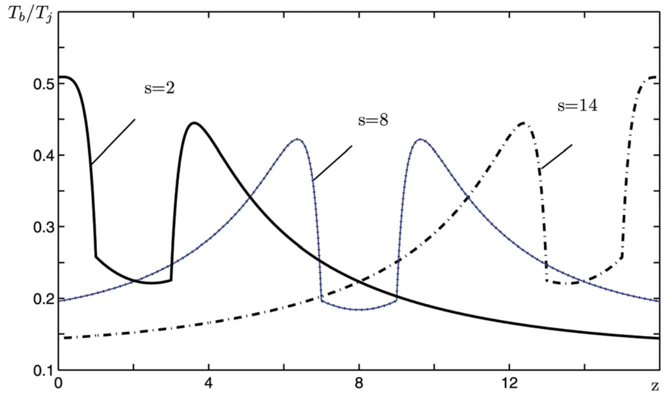

FIG. 9. (Color online) Stationary temperature distribution in the thermally insulated conductor T_b/T_j vs distance z from the left surface of the slab $z=0$, for different distances s between the center of the spherical inclusion and the left slab surface: $a=1, d=16, \rho=0, \chi=50, \kappa=33, \beta=0.3$.

(see Fig. 9), and temperature distribution varies less sharply than in the case of small χ when the inclusion is strongly cooled (see Fig. 10).

The magnitude of the characteristic temperature used for normalization of the obtained results in the present study is $T_j = j_0^2 a^2/\sigma_2\kappa_2$, $\kappa_2 = c_2\chi_2/v_2$. In the studies mentioned in Sec. I the characteristic temperature and electric current density vary in a wide range. For the majority of the alloys the electric conductivity, $\sigma \sim 10^8$Si/m, thermal conductivity, $\kappa \sim 10^2$ W/mK, and for the electric current density $j_0 \sim 10^5$ A/cm^2 which was attained in Refs. 4 and 5 the magnitude of T_j for metal alloys is of the order of $(a/m)^2 10^8$K, e.g., we obtain that $T_j \sim 1 - 100$ K when $a \sim 10^{-3} - 10^{-4}$ m.

V. CONCLUSIONS

We comprehensively studied the effect of inclusions on temperature distribution in current-carrying conductors. It was demonstrated that when the size of the inclusion is of the order of the size of the conductor, the temperature distribution is significantly different from that in the homogeneous conductor, and the inclusion can be either heated or cooled with respect to the host conductor. The effective cooling can be achieved in the case of a thermally insulated conductor (see

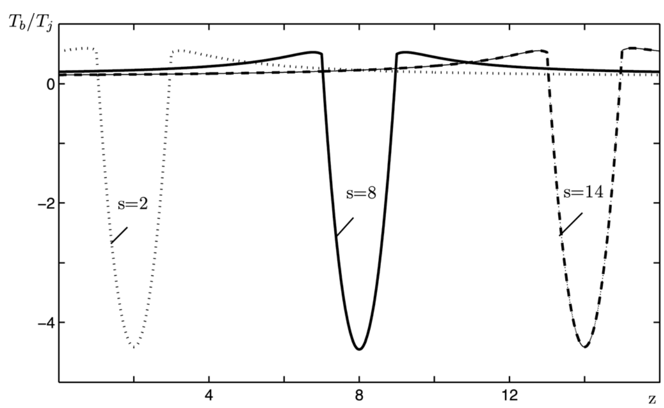

FIG. 10. Stationary temperature distribution in the thermally insulated conductor T_b/T_j vs distance z from the left surface of the slab $z=0$, for different distances s between the center of the spherical inclusion and the left slab surface: $a=1, d=16, \rho=0, \chi=0.05, \kappa=33, \beta=0.3$.

Figs. 9 and 10). In the regime when the surface temperature of the conductor is maintained constant, the inclusion is always heated (see Figs. 6–8). In the latter case, the magnitude of heating can be strongly affected by changing the parameters of the inclusion. The goal of this study was to investigate the effect of Joule heating on the temperature profile in a current-carrying conductor with an inclusion which is formed either during the phase transition or structural transformations, which were observed in Refs. 1–6 and 10.

The results obtained in this study imply that the strong reduction of crystallization temperature observed in Refs. 4 and 5 can be explained by the compensation of the heating which occurs during formation of a new phase. Elucidation of this aspect requires separate investigation of the phase transition in current-carrying conductors subjected to Joule heating. Although some aspects of this problem were analyzed in the literature, the multitude of regimes and processes involved render this problem a worthwhile subject for further study.

ACKNOWLEDGMENTS

We wish to thank an anonymous reviewer for numerous valuable comments and helpful suggestions that have improved the quality of our initial manuscript.

[1] A. K Misra, Metall. Trans. A **16A**, 1354 (1985); **17A**, 358 (1986).
[2] R. Takemoto. and H. Mizubayashi, Acta. Metal. Mater. **43**, 1495 (1995).
[3] H. Mizubayashi and S. Okuda, Phys. Rev. B **40**, 8057 (1989).
[4] J. P. Barnak, A. F. Sprecher, and H. Conrad, Scr. Metall. Mater. **32**, 879 (1995).
[5] H. Mizubayashi, N. Kameyama, T. Hao, and H. Tanimoto, Phys. Rev. B **64**, 054201 (2001).
[6] X. L. Wang, Y. B. Wang, Y. M. Wang, B. Q. Wang, and J. D. Guo, Appl. Phys. Let. **91**, 163112 (2007).
[7] Yu. Dolinsky and T. Elperin, Phys. Rev. B **47**, 14778 (1993).
[8] Yu. Dolinsky and T. Elperin, Phys. Rev. B **50**, 52 (1994).
[9] Yu. Dolinsky and T. Elperin, Phys. Rev. B **62**, 12656 (2000).
[10] F. C. S. da Silva, E. F. Ferrari, and M. Knobel, J. Appl. Phys. **86**, 7170 (1999).
[11] J. Happel and H. Brenner, *Low Reynolds Number Hydrodynamics* (Martunus Nihhoff, Dordrecht, The Netherlands, 1973).
[12] E. W. Hobson, *The Theory of Spherical and Ellipsoidal Harmonics* (Cambridge University Press, Cambridge, England, 1965).